Bulletin de la Société Royale des Sciences de Liège, Vol. 87, Actes de colloques, 2018, p. 253 - 256

Triggered star-formation in the NGC 7538 H II region

Saurabh Sharma*, Anil Kumar Pandey, Rakesh Pandey, Tirthendu Sinha

Aryabhatta Research Institute of Observational Sciences (ARIES), Nainital, 263 002, India

Abstract: We have generated a catalog of young stellar objects (YSOs) in the star forming region NGC 7538 using Hα and X-ray data. The spatial distribution of YSOs along with MIR, radio and CO emission are used to study the star formation process in the region. Our analysis shows that the O3V type high mass star 'IRS 6' might have triggered the formation of young low mass stars up to a radial distance of 3 pc.

1 Introduction

Massive stars have a strong effect on their surrounding environment creating wind-blown shells, cavities, and H II regions. On the one hand, the energy released through their stellar winds and radiation can disperse and destroy the remaining molecular gas and likely inhibits further star formation. On the other hand, in some circumstances, the same energy feedback can promote and induce subsequent star formation in the surrounding molecular gas (Koenig et al. 2012). The identification and characterization of the young stellar objects (YSOs) in star-forming regions (SFRs) hosting massive stars are essential steps to examine the physical processes that govern the star formation of the next generation in such regions. NGC 7538 is an H II region containing massive, main-sequence stars with spectral types between O3 and O9 (IRS 6 and IRS 5; Puga et al. 2010) ionizing the region, infrared (IR) sources IRS 1 (associated with a disc and an outflow; Sandell et al. 2009), IRS 2 and IRS 3 associated with UCH II regions and with the IR cluster NGC 7538S (Wynn-Williams et al. 1974, Sandell & Wright 2010), and YSOs like IRS 9 and IRS 11 (Werner et al. 1979). Thus, it is ideally suited to study the impact of massive stars on the formation of high- and low-mass stars in its surroundings.

2 The YSOs sample

We have identified 21 and 64 YSOs on the basis of their Hα emission and X-ray emission, respectively, using the data taken with the 1-m telescope of the Aryabhatta Research Institute of Observational Sciences (ARIES), the 2-m Himalayan Chandra Telescope (HCT), and the $Chandra$ X-ray telescope (see Sharma et al. 2017 for details). Multiwavelength data from the opical to the mid-IR (MIR) of these YSOs along with those which are identified on the basis of IR-excess emission (Ojha et al. 2004; Mallick et al. 2014; Chavarria et al. 2014) in the 15×15 arcmin^2 field around NGC 7538, are used for generating spectral energy distributions (SEDs). With a condition that they should have minimum data set of 5 points, these SEDs were analysed to derive individual physical properties of

*saurabh@aries.res.in

YSOs (463 sources, see Sharma et al. 2017 for details). Optical data of the YSOs were taken with the 1-m ARIES telescope and the near-IR (NIR)/MIR data were taken from 2MASS point source catalog (Skrutskie et al. 2006) and the available literature (Chavarria et al. 2014). The above YSOs were also classified according to their evolutionary status on the basis of α_{IRAC}, which is the slope of the SED based on data in the bands of the $Spitzer$ Infrared Array Camera (see Chavarria et al. 2014). Those which do not have α_{IRAC}, were classified on the basis of MIR and NIR Two Colour Diagrams (TCDs). If IRAC data is not available, then the NIR TCD classification scheme or the strength of Hα line were used to classify the sources (Sharma et al. 2017).

3 Triggered star formation

To study the mode of star formation in this region, in Fig. 1 (left panel), we have shown the spatial distribution of member YSOs superimposed on the 15×15 arcmin^2 8.0 μm IRAC image. Distributions of ionized gas as seen in the 1280 MHz radio continuum emission (green contours, Ojha et al. 2004), the ^{13}CO $J = 1 - 0$ line (magenta contour) and 850 μm continuum (white contour) emission maps taken from Chavarria et al. (2014) are also shown in Fig. 1 (right panel). The YSOs are distributed either on the nebulosity parts or towards the southern regions. The distribution of the ^{13}CO, 850 μm and radio emission indicates a bubble-like feature around the ionizing source IRS 6, likely created due to the expansion of the H II region. The correlation of the Polycyclic Aromatic Hydrocarbon (PAH) emission as seen in the IRAC 8.0 μm image with the ^{13}CO emission indicates that the ionized gas is confined inside the molecular cloud. The distribution of Class I YSOs shows a nice correlation with that of molecular gas and the PAH emission/H II region boundaries suggesting an enhanced star formation activity towards this region. There is a concentration of very young YSOs (mainly Class I) towards the southern region outside of the dust rim (IRS 11). Five high-mass dense clump candidates (Fallscheer et al. 2013) are located just outside the NGC 7538 H II region towards south-west. There are many separate groups of younger YSOs located near these cold molecular clumps.

The two rim-like structures with sharp edges (maybe due to the PAH emission) pointing towards the central star IRS 6 in Fig. 1 indicate that the ionization front (IF) interacts with the molecular ridge as seen in the ^{13}CO emission. They morphologically resemble bright-rimmed clouds that result from the pre-existing dense molecular clouds impacted by the ultraviolet (UV) photons from nearby OB stars and the low mass YSOs on their tips are generally believed to be formed as a result of a triggering effect of the expanding H II region (Lefloch & Lazareff 1994; Deharveng et al. 2009). The elongated distribution and age difference of these YSOs with respect to the ionization source can be used to check whether the radiation-driven implosion (RDI; Lefloch & Lazareff 1994) mode of triggered star formation was effective in the region. We have also compared the time elapsed during the formation of the Class I YSOs in these globules with the age/ lifetime of the O3 ionization source 'IRS 6'. The position of the tips of the globules is situated at a projected distance of $\sim$ 2.4 pc from IRS 6. We estimated the time needed for the IF to travel the distance as $\sim$ 0.26 Myr, assuming an expansion speed of $\sim$ 9 km s^{-1} (see, e.g. Pismis & Moreno 1976). The age of the Class I sources on this rim is 1.9 ± 0.6 Myr, which is $\sim$ 0.3 Myr younger than the approximate age of the O3V star ($\sim$ 2.2 Myr, cf. Puga et al. 2010). The mean age of the Class I sources inside the rim is 1.5 ± 0.6 Myr. We have estimated the shock crossing time in the globules to see whether the star formation there was initiated by the propagation of the shock or whether it had already taken place prior to the arrival of the shock. Assuming a typical shock propagation velocity of 1-2 km s^{-1}, as found in the case of bright-rimmed clouds (see, e.g., Thompson et al. 2004), the shock travel time to the YSOs, which are at a projected distances of $\sim$ 0.6 pc from the head, is $\sim$ 0.4 Myr. This time-scale is comparable to the difference in the ages of the YSOs on the rims and inside them. These results seems to support the notion that the formation of the YSOs in the globules could be due to the RDI mechanism. To investigate this

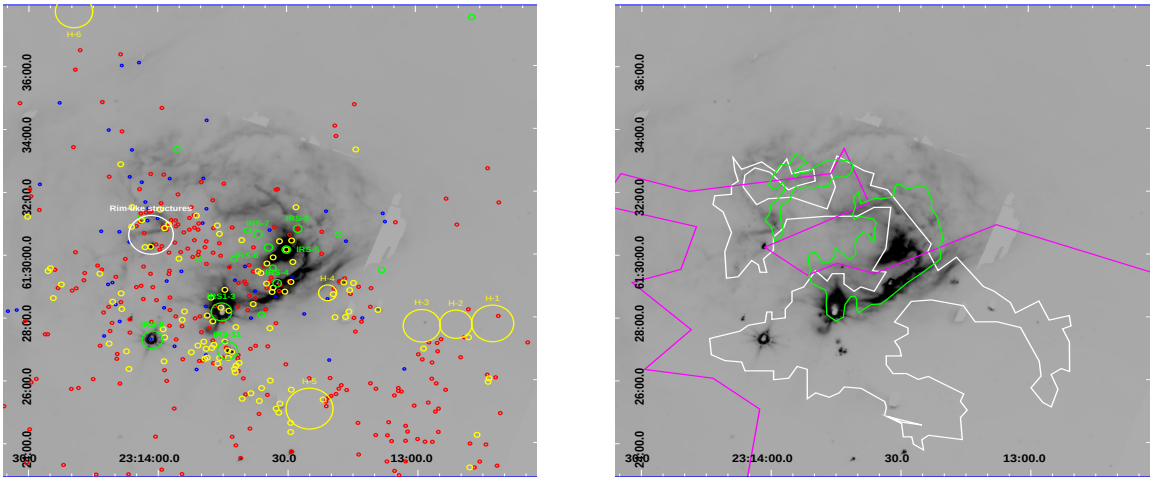

Figure 1: Left: Spatial distribution of the YSOs superimposed on the $15' \times 15'$ IRAC 8.0 μm image of the NGC 7538 region. The location of Class I (yellow dots), Class II (red dots), Class III (white dots), and unclassified (blue dots) sources are shown along with the IR sources (green circles) and the positions of high-mass dense clumps (yellow circles, Fallscheer et al. 2013). Right: Distributions of the ionized gas as traced by radio (1280 MHz, green contours, Ojha et al. 2004) are shown overlaid on the IRAC 8.0 μm image of the same region. The $J = 1 - 0$ line of ^{13}CO (magenta contour) and 850 μm continuum emission (white contour) taken from Chavarria et al. (2014) are also shown. The x-axis and y-axis in the figures are RA and Dec in J2000 epoch, respectively.

suggestion further, we have calculated the dynamical age of the NGC 7538 H II region from its radius using the equation given by Spitzer (1978): $R(t) = R_S(1 + \frac{7ct}{4R_s})^{4/7}$, where $R(t)$ denotes the radius of the H II region at time t, and c is the sound speed. The latter was assumed as $\sim$9 km s^{-1} (Pismis & Moreno 1976), and the former was taken to be 3 pc, as derived from the radio map (cf. Fig. 1). The dynamical age (t) can be calculated if we know the Strömgren radius R_S. It can be estimated by using the relation given in Ward-Thompson & Whitworth (2011) and Stahler & Palla (2005) and by assuming an O3V star as the ionizing source emitting 7.4 $\times 10^{49}$ UV photons per second (Vacca et al. 1996). However, as the information on the initial ambient density is not known, we have assumed it as a free parameter. The estimates for R_S and the corresponding dynamical age (t) of the H II region for ambient densities ranging from 10^3 to 10^4 cm^{-3} comes out to be $\sim$ 1.3 to 0.25 pc and $\sim$ 0.7 to 2.6 Myr, respectively. This upper limit of the dynamical age, is comparable to the age of the ionizing star IRS 6, and corresponds to a high ambient density for this region. The mean age of the YSOs in this region is 1.4 Myr, so they are younger than the dynamical age of the region. As such, their formation could have been influenced by the expanding H II region.

We have also studied the radial dependence of the extinction A_V, age, and mass of YSOs from the ionizing source IRS 6 in Fig. 2. As expected, the A_V distribution reveals less extinction near IRS 6 as compared to the outer region. There is a broad peak at the projected distance of $\sim$ 3 to 5 pc and we see a decreasing trend after that. This seems to indicate the presence of a shell-like layer of collected material just outside the H II region. The age and mass distribution show a decrease from the center to a radial distance of 3 pc indicating a difference in the physical properties of the YSOs within 3 pc to those outside. These trends are indicative of triggered star formation in the inner region (within 3 pc), where the O3 star played an active role. A completely different distribution with a large number of young and low mass YSOs are located in the south-west region of NGC 7538 at a radial distance beyond 3 pc. It seems that the YSOs in this group might have formed spontaneously in the absence of any triggering mechanism. The distribution of the cold clumps also suggests that spontaneous low-

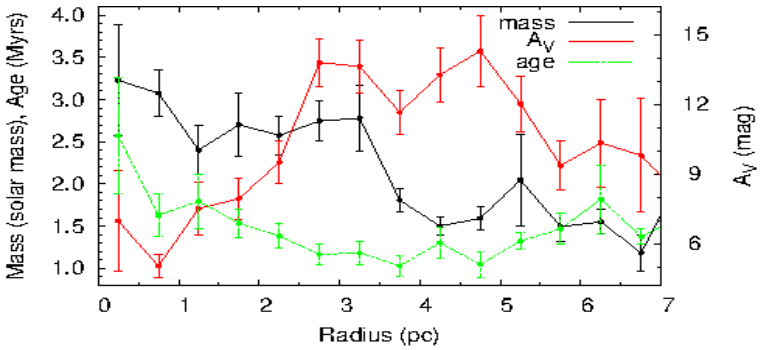

Figure 2: Distribution of the extinction A_V, age, and mass of the YSOs as a function of radial distance from the ionizing source IRS 6.

mass star formation is under way there. However, to disentangle the triggered population from the spontaneously formed population requires a precise determination of the proper motions and ages of the individual sources (Dale et al. 2015).

4 Conclusion

Although the NGC 7538 region has already been studied extensively at IR and radio wavelengths, it is rather neglected in the optical and X-ray region. We have added more YSOs on the basis of Hα or X-ray emission to the available catalogs of the YSOs in the region (Ojha et al. 2004; Mallick et al. 2014; Chavarria et al. 2014). The spatial distribution of the YSOs along with those of MIR/radio/CO emission has been used to understand the star formation process in this region. The YSOs in the inner region (within 3 pc from IRS 6, containing the bright H II region) might have been formed by a triggering mechanism caused by the central high mass star IRS 6.

References

Chavarria L., Allen L., Brunt C. et al. 2014, MNRAS, 439, 3719
Dale J. E., Haworth T. J., Bressert E. 2015, MNRAS, 450, 1199
Deharveng L., Zavagno A., Schuller F. et al. 2009, A&A, 496, 177
Fallscheer C., Reid M. A., Di Francesco J. et al. 2013, ApJ, 773, 102
Koenig X. P., Leisawitz D. T., Benford D. J. et al. 2012, ApJ, 744, 130
Lefloch B., Lazareff B. 1994, A&A, 289, 559
Mallick K. K., Ojha D. K., Tamura M. et al. 2014, MNRAS, 443, 3218
Ojha D. K., Tamura, M., Nakajima Y. et al. 2004, ApJ, 616, 1042
Pismis P., Moreno M. A. 1976, RMxAA, 1, 373
Puga E., Marin-Franch A., Najarro F. et al. 2010, A&A, 517, A2
Sandell G., Goss W. M., Wright M., Corder S. 2009, ApJ, 699, L31
Sandell G., Wright M. 2010, ApJ, 715, 919
Sharma S., Pandey A. K., Ojha D. K. et al. 2017, MNRAS, 467, 294
Skrutskie M. F., Cutri R. M., Stiening R. et al. 2006, AJ, 131, 1163
Spitzer L. 1978, Physical Processes in the Interstellar Medium. Wiley-Interscience, New York
Stahler S. W., Palla F. 2005, The Formation of Stars. Wiley-VCH, Weinheim
Thompson M. A., White G. J., Morgan L. K. et al. 2004, A&A, 414, 1017
Vacca W. D., Garmany C. D., Shull J. M. 1996, ApJ, 460, 914
Ward-Thompson D., Whitworth A. P. 2011, An Introduction to Star Formation. Cambridge Univ. Press, Cambridge
Werner M. W., Becklin E. E., Gatley I. et al. 1979, MNRAS, 188, 463
Wynn-Williams C. G., Becklin E. E., Neugebauer G. 1974, ApJ, 187, 473